Cancer Letters 460 (2019) 139–151

Contents lists available at ScienceDirect

Cancer Letters

journal homepage: www.elsevier.com/locate/canlet

Original Articles

CircNR3C1 inhibits proliferation of bladder cancer cells by sponging miR-27a-3p and downregulating cyclin D1 expression

Fuxin Zheng[a,b,1], Miao Wang[a,1], Yawei Li[c,1], Chao Huang[a], Dan Tao[d], Fei Xie[a], Hui Zhang[a], Jiayin Sun[a], Chuanhua Zhang[b], Chaohui Gu[e], Zhendi Wang[a,**], Guosong Jiang[a,*]

[a] Department of Urology, Union Hospital, Tongji Medical College, Huazhong University of Science and Technology, Wuhan, 430022, China
[b] Department of Urology, Wuhan No.1 Hospital, Tongji Medical College, Huazhong University of Science and Technology, Wuhan, 430022, China
[c] Department of Urology, The First Affiliated Hospital of Wannan Medical College, Wuhu, 241001, China
[d] Department of Oncology, The Fifth Hospital of Wuhan, Wuhan, 430050, China
[e] Department of Urology, The First Affiliated Hospital of Zhengzhou University, Zhengzhou, 450052, China

ARTICLE INFO

Keywords:
Bladder cancer
CircNR3C1
miR-27a-3p
Cyclin D1
5′UTR

ABSTRACT

Accumulating evidences suggest that circular RNAs play vital roles in human cancers. Previously, we found that circHIPK3 suppressed invasion of bladder cancer cells via sponging miR-558 and downregulating heparanase expression. In this study, we discovered that a circular RNA derived from NR3C1 (circNR3C1) was downregulated in bladder cancer tissues and cell lines according to RNA-Seq data and qRT-PCR analysis. Functionally, we found that overexpression of circNR3C1 could significantly inhibit cell cycle progression and proliferation of bladder cancer cells in vitro, as well as suppress tumor growth in vivo. Mechanistically, we demonstrated that circNR3C1 possessed four targeting sites of miR-27a-3p and could effectively sponge miR-27a-3p to suppress the expression of cyclin D1. Furthermore, we revealed that miR-27a-3p functioned as an oncogene through interacting with 5′UTR of cyclin D1 to enhance its expression, which led to promote cell cycle progression and proliferation in bladder cancer cells. Conclusively, our findings further confirm the hypothesis that circRNAs function as “microRNA sponges”, and our data suggest that circNR3C1 and miR-27a-3p would be potential therapeutic targets for bladder cancer treatment.

1. Introduction

Bladder cancer is one of the most frequently occurring malignancies of urinary system worldwide [1]. Both the incidence and mortality of bladder cancer have risen steadily in recent decades. Recent studies suggest that bladder cancer comprises a group of molecularly heterogeneous diseases which lead to various clinical features and possess diverse therapeutic responses [2]. Thus, development of precise strategies is worthy and important.

As a new type of RNAs, covalently closed circular RNA molecules (circRNAs) were originally discovered in plant viroids [3], hepatitis virus [4] and eukaryotic cells [5] more than 40 years ago. Subsequently, a handful circular RNAs were identified in human [6,7] and mouse [8], and were considered as by-products of aberrant splicing with little functional potential [9]. Next-generation RNA sequencing (RNA-Seq) from nonpolyadenylated RNA transcripts and bioinformatic analyses recently demonstrated that circRNAs were widely expressed in diverse mammalian cell lines and across various species [10–12]. Unlike known unidimensional lncRNAs, circRNAs in general were produced from pre-mRNAs back splicing events, which covalently linked the 3′ and 5′ ends of exons or introns together and formed single-stranded continuous loop structures with neither a 5′ cap nor a 3’ polyadenylated tail [13–16]. Compared to linear RNAs, circRNAs were much more resistant to RNase R and more stable, which was probably due to the absence of 5′ and 3′ ends [17]. Studies have revealed that circRNAs displayed some conservation, high abundance, cell type- or tissue- and developmental stage-specific expression [10,18]. Recently, the functions of circRNAs in regulating gene expression were reported by a series of investigations, and dozens of circRNAs have been shown to play important roles in human cancers including oral cancer [19], glioma [20], hepatocellular carcinoma [21], colorectal cancer [22] and bladder cancer [23].

* Corresponding author.
** Corresponding author.
E-mail addresses: wangzhendi@gmail.com (Z. Wang), jiangguosongdoc@hotmail.com (G. Jiang).
[1] These authors contributed equally to this work.

https://doi.org/10.1016/j.canlet.2019.06.018
Received 4 February 2019; Received in revised form 24 June 2019; Accepted 24 June 2019

MicroRNAs (miRNAs) which are just 19-22 bases in length are endogenous small noncoding RNAs that regulate the expression of protein-coding genes by direct base pairing to target sites within untranslated regions of mRNAs [24]. A growing body of evidences demonstrated that miRNAs produced great effects on bladder cancer genesis, development, progression, and metastasis [25]. Recently, miRNAs have been reported to be sponged by circRNAs, which function as competing endogenous RNAs to negatively regulate biofunctions of miRNAs [13]. It was reported that miR-29a could be sponged by *circMYLK*, which significantly contributed to bladder cancer progression [26]. Our previous study has verified that *circHIPK3* could sufficiently interact with miR-558 and subsequently suppressed metastasis and angiogenesis in bladder cancer [23]. However, the functions of other dysregulated circRNAs still need to be elucidated in human bladder cancer progression.

Previously, we have analyzed the expression profile of circRNAs in human bladder cancer tissues and paired normal tissues through High-Throughput Sequencing [23]. In the present study, we firstly confirmed that *circNR3C1*, which we also named it as bladder cancer related circular RNA-1 (*BCRC-1,* GenBank: KU921432.1), was downregulated in bladder cancer tissues and cell lines compared to normal tissues and urothelial cell line. Importantly, we found that *circNR3C1* could efficiently bind miR-27a-3p to suppress the expression of cyclin D1, and consequently inhibit cell proliferation and cell cycle progression of bladder cancer cells.

2. Methods and materials

2.1. Human tissue specimens

Tissue specimens of bladder cancer and paired adjacent normal bladder tissues were prepared as described [23]. Before we collected the samples, we have received the approval from the Institutional Review Board of Huazhong University of Science and Technology (Wuhan, China). All specimens were classified according to the 2004 World Health Organization Consensus Classification and TMN staging system for bladder neoplasms. Detailed Clinicopathological features were shown in Supplementary Table 1.

2.2. Cell culture and treatments

The human metastatic bladder cancer cell line T24T, which is a lineage-related lung metastatic variant of invasive bladder cancer cell line T24 [27], was provided by Dr. Dan Theodorescu (Departments of Urology, University of Virginia, Charlottesville, VA). Human bladder cancer cell lines EJ, UMUC3, J82, 5637 and human immortalized uroepithelium cell line (SV-HUC-1) were purchased from American Type Culture Collection (ATCC, USA). All the cell lines were cultured in F-12K medium (Gibco, China) supplemented with 10% fetal bovine serum (Gibco) and 1% penicillin/streptomycin (Gibco) and maintained at 37 ˚C in a humidified atmosphere with 5% CO2.

2.3. Nucleic acid preparation, RNase R treatment and real time PCR

Genomic DNA (gDNA) was isolated with QIAamp DNA Mini Kit (QIAGEN, Germany). Total RNA from tissue specimens and cell lines was extracted using RNeasy Mini Kit (QIAGEN, Germany) following the manufacturer's instructions. For RNase R treatment, total RNA was incubated 15 min at 37 ˚C with or without 3 U/mg of RNase R (Epicenter, WI, USA). The RNA treated with RNase R was subsequently purified using RNeasy MinElute cleaning Kit (Qiagen). Complementary DNA (cDNA) was synthesized using the PrimeScript RT Master Mix (Takara, Dalian, China) from 500 ng of RNA with random or oligo (dT) primer. For detection of circRNAs, mRNAs and miRNAs expression levels, the quantitative real-time PCR analyze (qRT-PCR) was performed using SYBR Premix Ex Taq™ kit (Takara) and StepOnePlus Real-Time PCR System (Applied Biosystems, Carlsbad, CA, USA). The values of $2^{-\Delta\Delta CT}$ relative to one of the samples were calculated to analyze relative expression levels of the RNAs. *GAPDH* was used to normalize the relative expression levels of circRNAs and mRNAs, and *RNU6-1* was used to normalize the relative expression levels of miRNAs. All the primers are listed in Supplementary Table 2.

2.4. PCR amplification and sanger sequencing

cDNA and gDNA templates were amplified using PCR Master Mix (2 ×) (Thermo Fisher Scientific, Waltham, MA, USA) following the manufacturer's protocol for 38 cycles. The PCR products were observed and acquired under ultraviolet after electrophoresis in 1%–3% GelGreen™ (Biotium, CA, USA) stained agarose gel. Subsequently, the PCR products were extracted by E.Z.N.A.® Gel Extraction Kit (Omega Bio-tek, Inc., USA), and were sent to TsingKe Biological Technology (Beijing, China) for sanger sequencing. The Primers for Sanger sequencing were provided in Supplementary Table 2.

2.5. Northern blotting

Digoxigenin (DIG)-labeled *circNR3C1* or *NR3C1* probes were prepared with DIG Labeling Kit (MyLab Corporation, Beijing, China) according to the manufacturer's instructions. Total RNA (5ug) extracted from *circNR3C1* plasmid or vector transfected cells (EJ and T24T) and DIG-labeled RNA molecular weight marker (Roche, USA) were loaded on a 1.2% agarose gel with 1% formaldehyde and run for 1 h in MOPS buffer. The gel was soaked in 10 × SSC for 10 min, and the RNA was transferred onto Hybond-N + membranes (GE Healthcare, USA) by capillary transfer overnight. Membranes were washed, and the RNA was fixed onto the membrane by UV cross-linker (UVP, CA, USA) for 15 min. Pre-hybridization was carried out at 72 ˚C for 1 h and hybridization was performed with DIG-labeled *circNR3C1* probe at 72 ˚C overnight. The membranes were briefly washed twice in 2 × SSC and 0.1% SDS at room temperature and washed stringently two additional times in 0.1 × SSC and 0.1% SDS at 55 ˚C for 30 min. The detection was carried out using DIG colorimetric detection kit (MyLab, China) following the manufacturer's instructions. Images were taken in natural night with digital camera (Nikon, Japan). The probe sequences are listed in Supplementary Table 2.

2.6. Plasmids construction and transfection

CircNR3C1 over-expression plasmid was constructed by TSINGKE (Beijing, China) based on pcD-ciR vector, which contained a front circular frame and a back circular frame [23]. To construct Luciferase reporter vectors of human cyclin D1 5′UTR, the 5′ UTR cDNA of cyclin D1 was prepared using PCR amplification, and was cloned into pGL3.0-control vector between HindIII and NcoI digest sites. The mutants of cyclin D1 5′UTR were provided by TSINGKE (Beijing, China). Cell lines were transfected using Lipofectamine 2000 (Life Technologies, USA) according to the manufacturer's instructions. Stable cell lines were established by treatment of G418 (Life Technologies, Carlsbad, CA, USA) for about 4 weeks. The primers for constructing plasmids were listed in Supplementary Table 2.

2.7. RNA fluorescence in situ hybridization (FISH)

Cy3-labeled *circNR3C1* and Fam-labeled miR-27a-3p probes were obtained from RiboBio (Guangzhou, China). Hybridizations were carried out using Fluorescent in Situ Hybridization Kit (RiboBio, China) according to the manufacturer's instructions. All fluorescence images were captured using Nikon A1Si Laser Scanning Confocal Microscope (Nikon Instruments Inc, Japan).

2.8. Pull-down assay with biotinylated circNR3C1 probe

The biotinylated probe of *circNR3C1* which was complemented to the back-splicing junction of *circNR3C1* was synthesized by TSINGKE (Beijing, China). The sequence of *circNR3C1* probe was listed in Supplementary Table 2. Pull-down assay was performed as described [23]. Briefly, about 1×10^7 bladder cancer cells which were transfected with vector or *circNR3C1* over-expression plasmid were harvested, crosslinked, lysed, and sonicated. The cell lysates were incubated with appropriate *circNR3C1* probe or oligo probe at 37 °C for 4 h in Hybridization Buffer. Subsequently, the lysates with or without *circNR3C1*-probe complex were incubated with appropriate C-1 magnetic beads (Life Technologies) for 30 min. Then, the beads were washed thoroughly with wash buffer, and the RNA complexes combining on the beads were isolated with RNeasy Mini Kit (QIAGEN, China) for RT–PCR or qRT-PCR.

2.9. Pull-down assay with biotinylated miR-27a-3p

This experiment was performed as previous report described [28]. The biotinylated miR-27a-3p probe was synthesized by RiboBio (China). Briefly, wild type and mutant type of biotinylated miR-27a-3p (50 nM) were transfected into EJ and T24T cells using Lipofectamine RNAiMax. After 48 h of transfection, the cells were harvested and sonicated. Then, 10 μl of the cell lysates were sucked out for input, and the remaining lysates were incubated with C-1 magnetic beads (Life Technologies) at 4 °C overnight. Next, the beads were washed with wash buffer, and the RNAs captured by beads were extracted using RNeasy Mini Kit (QIAGEN). Finally, qRT-PCR was performed to detect relative *circNR3C1* expression level. The sequences of biotin-miR-27a-3p probes were listed in Supplementary Table 2.

2.10. Western blotting

The total proteins were prepared and their concentrations were detected as we previously described [23]. Antibodies against CDK2 (Cat. No: 10122-1-AP), CDK4 (Cat No: 11026-1-AP), CDK6 (Cat. No: 14052-1-AP), cyclin D1(Cat. No: 60186-1-Ig), cyclin E (Cat. No: 11554-1-AP), P21 (Cat. No: 10355-1-AP), P27 (Cat. No: 25614-1-AP), β-actin (Cat. No: 60008-1-Ig), HRP-conjugated secondary goat anti-mouse (Cat. No: SA00001-1) and goat anti-rabbit (Cat. No: SA00001-2) antibodies were purchased from Proteintech Group (Rosemont, IL, USA). Immunoreactive bands were detected using the Immobilon ECL substrate kit (Millipore, Merck KGaA, Germany). The images were acquired by using BioSpectrum 600 Imaging System (UVP, CA, USA). The grey values were calculated using Image J 1.46r software, and β-actin was used as protein loading control.

2.11. Cell Counting Kit-8(CCK-8) assay

The cell viability was detected by Cell Counting Kit-8 assay (Dojin, Japan). Cells were starved in medium with 0.1% fetal bovine serum for 24 h. Next, approximately 2×10^3 cells were evenly seeded in 96-well plates in triplicate. Then, CCK-8 solution (10 μl) was added into each well and incubated at 37 °C for 2.5 h. The OD value at 450 nm was measured using the SpectraMax M5 microplate reader (MD, USA) at 0, 24, 48 and 72 h, respectively. The cell doubling times were calculated using GraphPad Prism 6.0 software (La Jolla, USA), and the OD values were used to perform statistics analysis.

2.12. 5-Ethynyl-20-deoxyuridine (EdU) assay

The EdU assay was carried out using Cell-Light EdU DNA Cell Proliferation Kit (C10310-1, RiboBio Guangzhou, China) according to the manufacturer's protocol. Images were acquired with an Olympus FSX100 microscope (Olympus, Tokyo, Japan). The cell proliferation rate was calculated as described [29].

2.13. Colony formation assay

Cells were seeded in 6-wells plates at density of 500 cells per well, and EJ and T24T cells were incubated for 7 days and 8 days, respectively. Then, the cell colonies were fixed with 4% paraformaldehyde and stained using dyeing solution containing 0.1% crystal violet. Cell colonies with more than 50 cells were counted.

2.14. Soft agar colony formation assay

The Soft Agar Colony Formation Assay was performed as we previously described [30]. Images were acquired using an Olympus FSX100 microscope (Olympus, Tokyo, Japan). Colonies with more than 50 cells were counted and presented as colonies per 10^4 cells.

2.15. Cell cycle assay

Cells were harvested and fixed with 75% ethanol overnight. The fixed cells were washed with PBS twice and mixed with the reagent from propidium iodide (PI) cell cycle detected kit (BD Pharmingen, NJ, USA). Then, the cell cycle analysis was performed by Myhalic Biotech (Wuhan, China).

2.16. Tumor xenografts experiments

The tumor xenografts experiments were permitted by the Animal Care Committee of Tongji Medical College and performed as described in our previous studies [23]. EJ cells stably transfected with *circNR3C1* or control vector were subcutaneously injected into the nude mice. Then, the mice were maintained for three weeks before being sacrificed. The tumor weight and volume were recorded every 5 days, respectively.

2.17. Immunohistochemistry

Immunohistochemistry was performed by ServicBiotech (Wuhan, China). Images were obtained with an Olympus FSX100 microscope (Olympus, Japan). Protein expression levels were analyzed by calculating the integrated optical density per stained area (IOD/area) using Image-J 1.46r software.

2.18. Luciferase reporter assay

EJ and T24T cells were seeded in 24-well plates at a density of 5×10^3 cells per well and maintained for 24 h. Subsequently, 250 ng Firefily Luciferase (FL) and 500 ng Renilla luciferase reporter vectors (pRL-TK) were co-transfected with *circNR3C1* plasmid/vector or miRNA inhibitor/inhibitor NC into the cells for 48 h. The luciferase activity was measured with a dual luciferase reporter assay detection kit (Promega, WI, USA) on an Omega device (Omega, USA).

2.19. Statistical analysis

All the data was analyzed using GraphPad Prism 6.0 software (La Jolla, USA), and were indicated as means ± standard error of the mean (SEM). Parametric pared *t*-test was performed to compare the difference between bladder cancer tissues and paired normal tissues. Chi-squared Test was used to analyze the correlation between Clinicopathological features of bladder cancer patients and *circNR3C1* expression. One-way analysis of variance was performed to evaluate the group difference. $P < 0.05$ was used as the significant criteria.

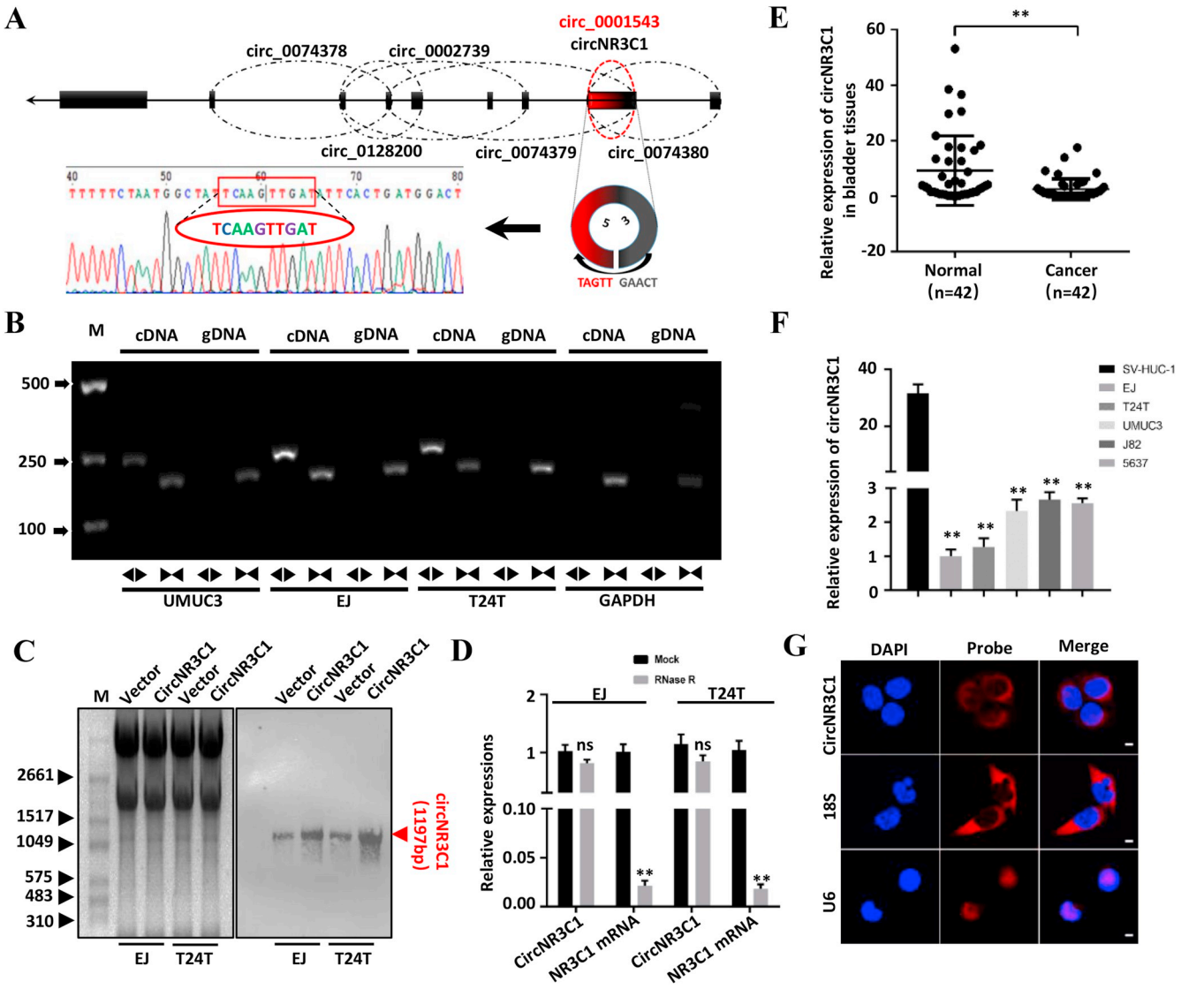

Fig. 1. Identification of *circNR3C1* and detection of its expression in bladder cancer tissues and cell lines. (A) Schematic diagram showed the circRNAs derived from *NR3C1* and the circularization of NR3C1 exon 2 formed *circNR3C1*. The presence of *circNR3C1* was confirmed by PCR amplification and followed by Sanger sequencing. (B) The existence of *circNR3C1* was verified in EJ, T24T and UMUC3 cells by RT–PCR. Divergent primers could amplify *circNR3C1* in cDNA but not genomic DNA (gDNA). *GAPDH* was used as linear control. (C) Northern blots were performed to detect *circNR3C1* in EJ and T24T cells transfected with *circNR3C1* or vectors. The left panel displayed the gel electrophoretic results of total RNA and the right panel showed the probed blots of *circNR3C1* (red triangle). (D) The expression of *circNR3C1* and *NR3C1* mRNA were measured using qRT-PCR in total RNA samples from EJ and T24T cells which were treated with RNase R or without RNase R (mock). The relative expression levels of *circNR3C1* and *NR3C1* mRNA were calculated using ΔΔCT method. Data indicate mean ± SEM, n = 3, $^{**}P < 0.01$ versus mock, ^{ns} p > 0.05 versus mock. (E) The relative expression of *circNR3C1* was detected using qRT-PCR in 42 pairs of bladder cancer tissues and paired normal bladder tissues. *GAPDH* was used as endogenous control. Data indicate mean ± SEM, n = 3, $^{**}P < 0.01$ versus normal bladder tissues. (F) The relative expression of *circNR3C1* was detected using qRT-PCR in SV-HUC-1, EJ, T24T, UMUC3, J82 and 5637 cells. *GAPDH* was used as endogenous control. Data indicate mean ± SEM, n = 3, $^{**}P < 0.01$ versus SV-HUC-1. (G) FISH assay showed that *circNR3C1* was mainly localized in cytoplasm. 18S was mostly localized in cytoplasm and used as positive control. *RNU6-1* was largely localized in nucleus and used as negative control. *circNR3C1*, 18S and *RNU6-1* probes were tagged with cy3, and nucleus was dyed with DAPI. Scale bar, 10 μm.

3. Results

3.1. CircNR3C1 is down-regulated in bladder cancer tissues and cell lines, and mainly localizes in cytoplasm

According to the RNA-seq data [23], we found that *circNR3C1*, which is named hsa_circ_0001543 in CircBase (http://www.circbase.org/), was down-regulated in bladder cancer tissues in comparison to paired normal tissues. *NR3C1* gene (GenBank: NM_001018074) could generate six different circRNAs in human, while *CircNR3C1* consists of the head-to-tail splicing of the exon-2 (Fig. 1A). To identify the existence of *circNR3C1* in bladder cancer cells, we used PCR to amplify distinct products of the expected size with divergent primers that were specially designed for detecting *circNR3C1,* and confirmed it using Sanger Sequencing (Fig. 1A). Nevertheless, head-to-tail splicing might be produced by reverse transcriptase template switching, *trans*-splicing and genomic rearrangements [31]. To rule out these possibilities, we designed two sets of primers for exon-2 from *NR3C1*, the convergent primers for amplifying linear form and the divergent primers for amplifying circular form. The results showed that the circular form only could be amplified in cDNA, but not in gDNA (Fig. 1B). Subsequently, we carried out northern blot analysis for *circNR3C1*. As shown in Fig. 1C, one distinct band of expected size (1197 bp) was detected by DIG-labeled *circNR3C1*-specific probe in EJ and T24T cells, while the

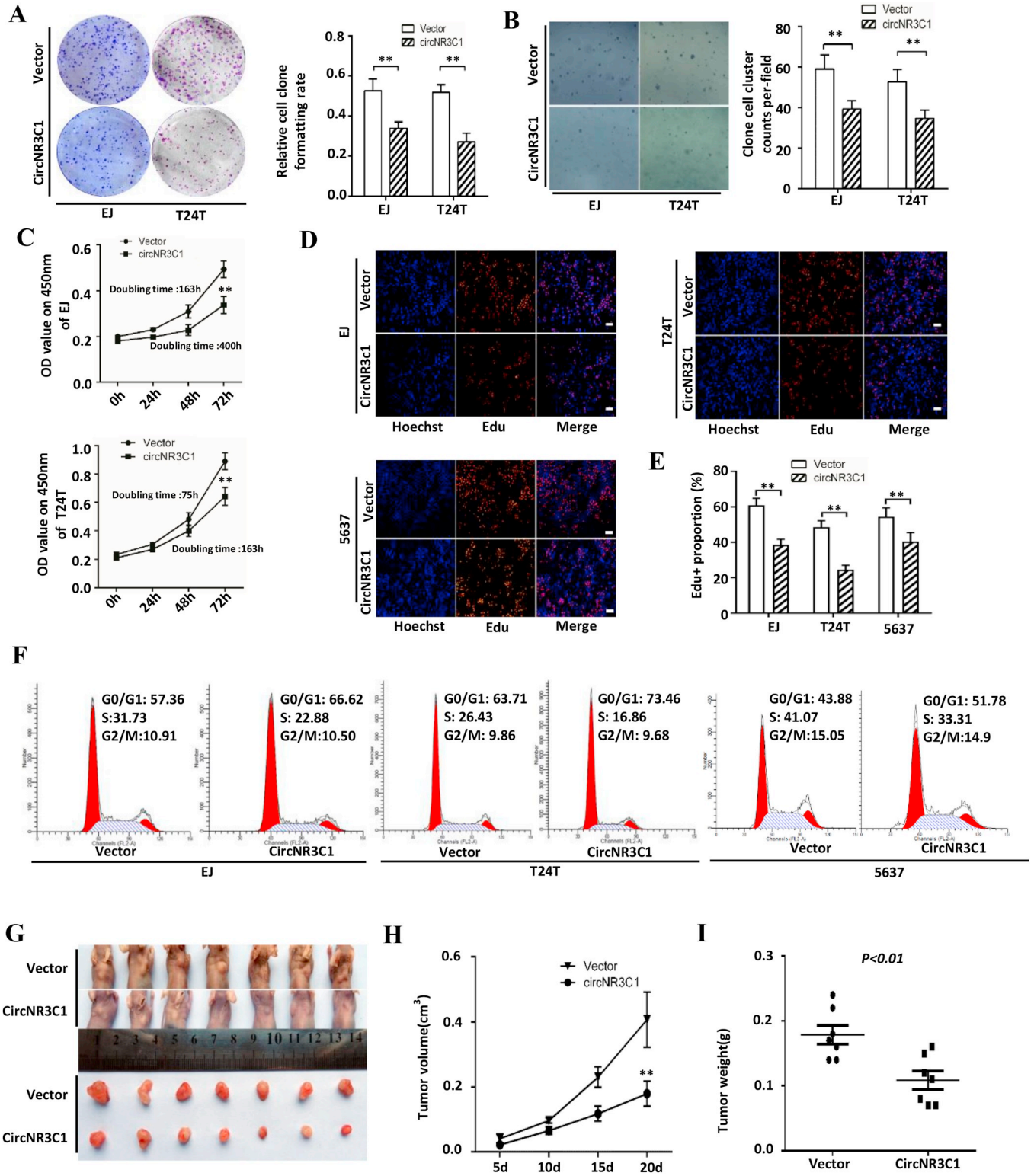

Fig. 2. Effects of *circNR3C1* on cell cycle progression and proliferation of bladder cancer cells. (A) EJ and T24T cells were treated with medium containing either vector or *circNR3C1* plasmid up to 48 h for colony formation assay. The ratio of cell clusters to total cells per well were calculated for statistical analysis. Data were presented as mean ± SEM. n = 3, $^{**}P < 0.01$. (B) Anchorage-independent growth were determined after EJ and T24T cells were transfected with *circNR3C1* or vectors for a week for soft agar assay. The counts of cell clusters per field were calculated for statistical analysis. Data were presented as means ± SEM, n = 3, $^{**}P < 0.01$. (C) CCK-8 assay was performed after stably transfected EJ and T24T cells were seeded in 96-well plate for 0 h, 24 h, 48 h, and 72 h and the cell doubling times were calculated. Data were mean ± SEM, n = 3, $^{**}P < 0.01$ versus vector group. **(D, E)** Cell proliferation activities were measured using EdU (5-ethynyl-2′-deoxyuridine) assay after EJ, T24T and 5637 cells were transfected with vector or *circNR3C1* for 48 h. Data were mean ± SEM, n = 3, $^{**}P < 0.01$. Scale bar, 200 μm. **(F)** Cell cycle were performed using flow cytometry after EJ, T24T and 5637 were transfected with *circNR3C1* or vectors for 48 h. The data were derived from three independent experiments. **(G–I)** EJ cells stably transfected with *circNR3C1* plasmid or vector were injected subcutaneously into BALB/c nude mice and established subcutaneous xenograft tumors (5×10^6 cells per mice, each group contains 7 mice). The tumor growth curve and weight were decreased in *circNR3C1*-treated group compared to vector group. Data were presented as mean ± SEM, $^{**}P < 0.01$ versus vector group.

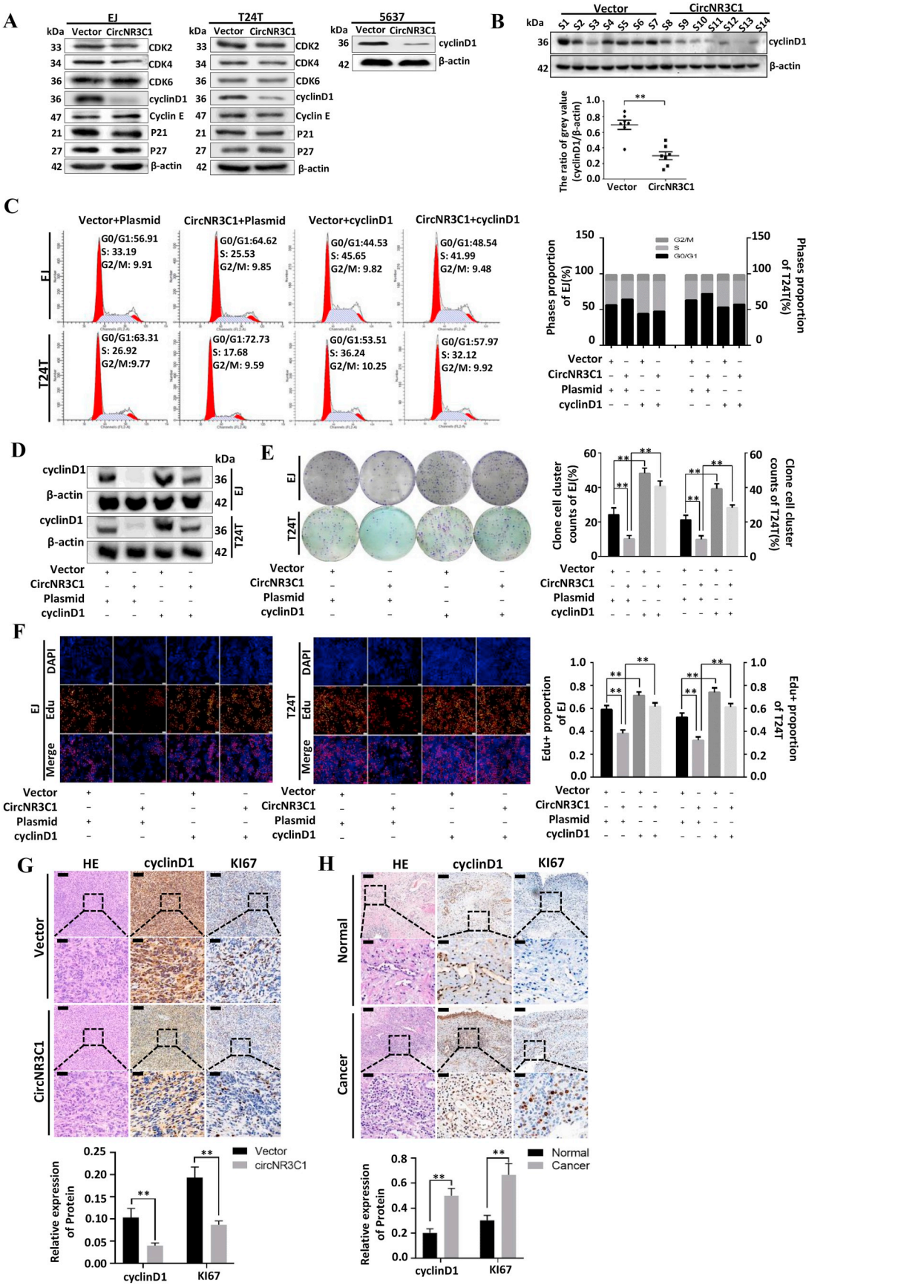

(caption on next page)

Fig. 3. *circNR3C1* inhibits cell cycle progression and proliferation through suppressing expression of cyclin D1. (A) The expressions proteins including CDK2, CDK4, CDK6, cyclin D1, CCNE1, P21 and P27 were detected using western blot in EJ, T24T and 5637 cells. Proteins were extracted after *circNR3C1* or vectors were stably transfected into the cells. β-actin was used as internal control. The results were derived from three independent experiments. (B) The protein expression levels of *cyclin D1* in xenograft tumors were detected using western blot, and grey values were calculated using ImageJ 1.46r to quantify the proteins. β-actin was used as internal control. S1-S7 were injected with vector stably transfected EJ cells and S8-S14 were injected with *circNR3C1* stably transfected EJ cells. The ratio of grey values (cyclin D1 to β-actin) was calculated to perform statistics. The results were derived from three independent experiments. Data were presented as mean ± SEM, $^{**}P < 0.01$. (C) Cell cycles were analyzed using flow cytometry in bladder cancer cells which were co-transfected with cyclin D1 controls (plasmid) or cyclin D1 plasmid, and *circNR3C1* controls (vector) or *circNR3C1* plasmid for 48 h. The results were derived from three independent experiments. (D) Western blot was performed to detect the expression of cyclin D1 in EJ and T24T cells which were transfected with cyclin D1 controls (plasmid) or cyclin D1 plasmid, and *circNR3C1* controls (vector) or *circNR3C1* plasmid. β-actin was used as internal control. The results were derived from three independent experiments. (E) Colony formation assay showed the colony formation efficiency of EJ and T24T cells which were co-transfected with cyclin D1 controls (plasmid) or cyclin D1 plasmid, and *circNR3C1* controls (vector) or *circNR3C1* plasmid for 48 h. The data indicated mean ± SEM, n = 3, $^{**}P < 0.01$. (F) EdU assay showed the proliferation of EJ and T24T cells which were co-transfected with cyclin D1 controls (plasmid) or cyclin D1 plasmid, and *circNR3C1* controls (vector) or *circNR3C1* plasmid for 48 h. The data indicated mean ± SEM, n = 3, $^{**}P < 0.01$. Scale bar, 200 μm. (G) Immunohistochemical staining shown that over-expression of *circNR3C1* led to decreased expression of cyclin D1 and Ki67 within tumors. The results were derived from three random staining fields of each section. The data indicated mean ± SEM, n = 3, $^{**}P < 0.01$. Scale bars, 10 and 100 μm. (H) Immunohistochemical staining revealed that protein levels of cyclin D1 and Ki67 were significantly upregulated in bladder cancer tissues compared to normal bladder tissues. The results were derived from three representative staining fields of each section. The data indicated mean ± SEM, n = 3, $^{**}P < 0.01$. Scale bars,10 and 100 μm.

signals from *circNR3C1* over-expression groups were more intensive in comparison to vector control groups. Furthermore, we confirmed that circNR3C1 was far more resistant to RNase R than the linear NR3C1 mRNA (Fig. 1D).

Then, relative expression levels of *circNR3C1* were detected in 42 pairs of bladder cancer tissues and adjacent normal bladder tissues using qRT-PCR. It demonstrated that *circNR3C1* was down-regulated in bladder cancer tissues comparing to paired normal tissues (Fig. 1E). However, the lower expression of *circNR3C1* was not correlated to the clinical indicators including bladder cancer grade and pathological stage (Supplementary Table 1). Consistent with the results from tissues, down-regulation of *circNR3C1* was also found in bladder cancer cell lines (EJ, T24T, UMUC-3, J82 and 5637) compared with human immortalized uroepithelium cells (SV-HUC-1) (Fig. 1F). To rule out the aberrant expression of *circNR3C1* caused by *NR3C1* mRNA expression, we further detected the levels of *NR3C1* mRNA transcripts in bladder cancer tissues and cell lines. The results showed that there was no significant difference on *NR3C1* mRNA expression between bladder cancer tissues and normal bladder tissues, as well as between SV-HUC-1 and bladder cancer cell lines (Figs. S1D and F). To obtain cell distribution of *circNR3C1*, RNA fluorescence in situ hybridization (FISH) assay was performed, and it demonstrated that *circNR3C1* mainly located in cytoplasm (Fig. 1G).

3.2. Overexpression of circNR3C1 inhibits proliferation and cell cycle progression of bladder cancer cells both in vitro and vivo

To explore the functions of *circNR3C1* in bladder cancer, *circNR3C1* overexpression plasmid was stably transfected into EJ, T24T and 5637 cells (Fig. S1A). Cell colony formation assay showed that colony-forming abilities of *circNR3C1*-overexpressed bladder cancer cells were lower than the control vector-transfected cells (Fig. 2A). The similar results were obtained from soft agar colony-formation assay (Fig. 2B). Consistently, CCK-8 cell viability assay and EdU assay demonstrated that stable transfection of *circNR3C1* resulted in decreased proliferation of bladder cancer cells in vitro (Fig. 2C, D, and 2E). Meanwhile, cell cycle assay indicated that overexpression of *circNR3C1* induced cell cycle arrest at G0/G1 phase in bladder cancer cells (Fig. 2F). We further transfected siRNAs targeting the junction sites of *circNR3C1* into EJ and T24T cells, and the EdU assay and clone formation experiments showed that the activities of bladder cancer cell proliferation were increased (Figs. S2A–B). Cell cycle assay indicated that knockdown of *circNR3C1* could promote cell cycle progression from G0/G1 phase to S phase (Fig. S2C). Over all, it appeared that the metastatic T24T cells are more responsive to *circNR3C1* than EJ and 5637 cells, indicating that *circNR3C1* might be a potential therapeutic target especially in metastatic bladder cancer. On the other hand, overexpression of *circNR3C1* didn't affect bladder cancer cell migration and invasion abilities (Fig. S2D), and couldn't induce cell apoptosis (Fig. S2E).

To further explore the biofunctions of *circNR3C1* in vivo, EJ cells stably transfected with control vector or *circNR3C1* overexpression plasmid were respectively inoculated into female nude mice. It showed that overexpression of *circNR3C1* could reduce the tumor volume and weight (Fig. 2G–I). Taken together, these results demonstrated that *circNR3C1* played an anti-oncogenic role via preventing cell cycle progression and inhibiting proliferation in bladder cancer.

3.3. CircNR3C1 induces G0/G1 stage of cell cycle arrest and inhibits cell proliferation through suppressing expression of cyclin D1

To clarify the molecular mechanisms underlying *circNR3C1* inhibition of cell proliferation and cell cycle progression, expression of cell cycle related proteins including CDK2, CDK4, CDK6, cyclin D1, CCNE1, cyclin dependent kinase inhibitor 1 A (P21, CDKN1A) and Cyclin-Dependent Kinase Inhibitor 1 B (P27, Kip1) were detected by western blot assays in *circNR3C1* stably transfected EJ and T24T cells, as well as in xenografts from mice. The results indicated that the protein expression levels of cyclin D1 were dramatically decreased in *circNR3C1*-overexpressed bladder cancer cells and the tissues, while the other proteins showed no change (Fig. 3A–B). To further confirm the role of *circNR3C1* in regulating cyclin D1 expression, we co-transfected *circNR3C1* overexpression plasmid and cyclin D1 overexpression plasmid into EJ and T24T cells. The cell cycle analysis showed that enforced expression of cyclin D1 could partially reversed cell cycle arrest at G0/G1 phase induced by *circNR3C1* (Fig. 3C). Meanwhile, western blot assay showed that the expression of cyclin D1 was significantly increased in the cells co-transfected with *circNR3C1* and *compared* with the cells co-transfected with *circNR3C1* and control vector (Fig. 3D). In addition, colony formation assay and EdU assay revealed that decrease of proliferation caused by *circNR3C1* could partly be reversed by overexpression of cyclin D1 (Fig. 3E–F). Immunohistochemical staining also showed that the expression of cyclin D1 and Ki67 was inhibited by overexpression of *circNR3C1* (Fig. 3G). In consistent with these results, cyclin D1 and Ki67 protein levels were upregulated in human bladder cancer tissues compared with normal bladder tissues (Fig. 3H). Collectively, these findings indicated that *circNR3C1* could induce G0/G1 arrest of bladder cancer cells through suppressing the expression of cyclin D1, and subsequently inhibited the proliferation of bladder cancer cells both in vitro and in vivo.

3.4. CircNR3C1 interacts with miR-27a-3p and miR-23a-3p in bladder cancer cells

Previous studies have reported that circRNAs could influence

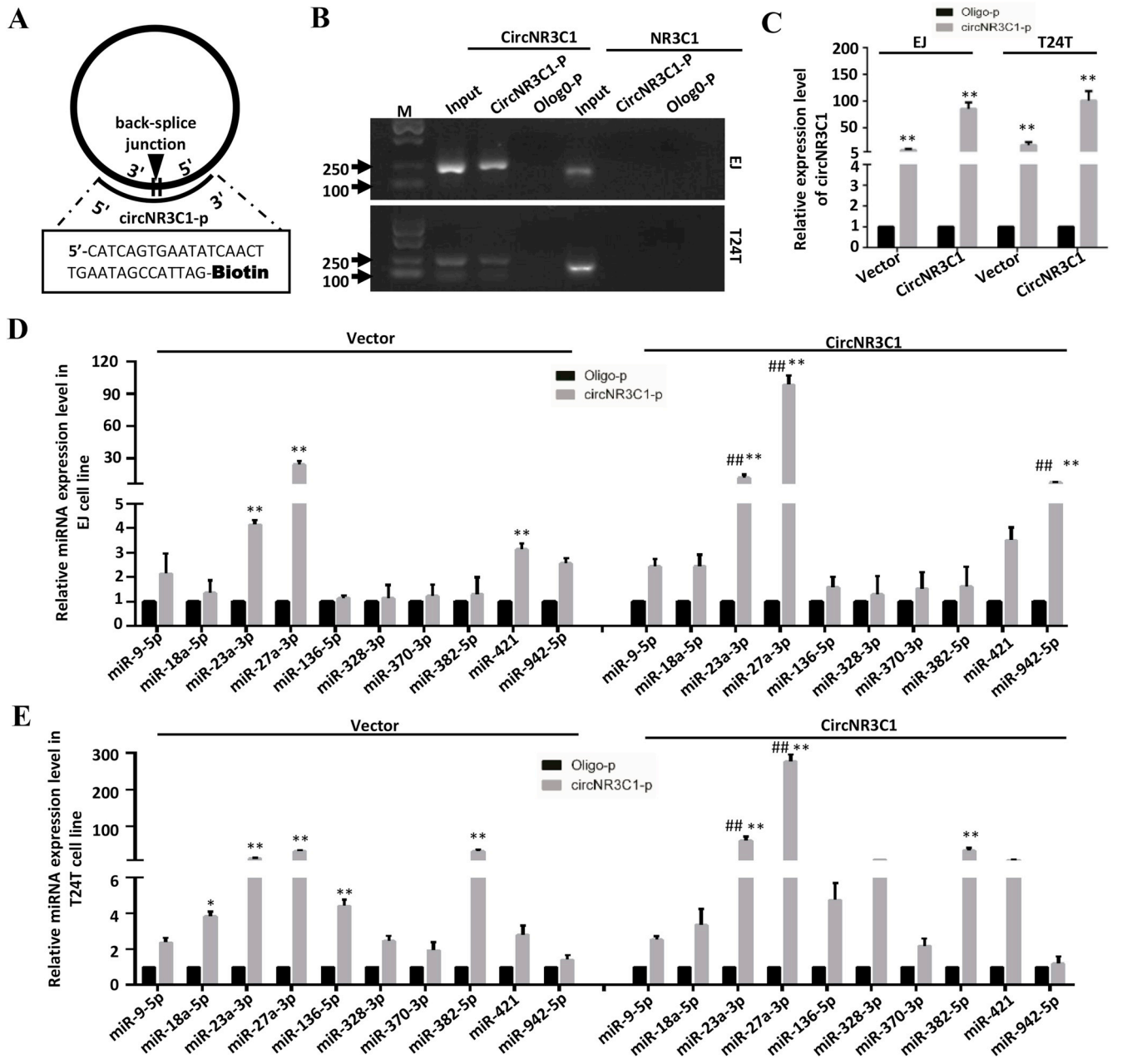

Fig. 4. *circNR3C1* interacts with miR-27a-3p and miR-23a-3p in bladder cancer cells. (A) Schematic diagram displayed the probe specifically designed for *circNR3C1*. (B) RT-PCR and gel electrophoretic results showed that *circNR3C1* probe could specifically pull down circular form of *circNR3C1* and couldn't pull down linear form. (C) Lysates were prepared from EJ and T24T cells transfected with *circNR3C1* plasmid or vector and were subjected to RNA pull-down assay. The expression of *circNR3C1* were tested by qRT-PCR and the relative expression level of *circNR3C1* was normalized to input. Data indicated mean ± SEM, n = 3, $^{**}P < 0.01$ versus oligo probe (Oligo-p). (D) The relative expression level of 11 miRNA candidates was detected by qRT-PCR in lysates from *circNR3C1* or vectors-transfected EJ cells. Data indicated mean ± SEM, n = 3, $^{**}P < 0.01$ versus oligo probe, $\#\#P < 0.01$ versus vector group. (E) The relative expression levels of 11 miRNA candidates was detected using qRT-PCR in lysates from *circNR3C1* or vectors-transfected T24T cells. Data indicated mean ± SEM, n = 3, $^{*}P < 0.05$, $^{**}P < 0.01$ versus oligo probe, $\#\#P < 0.01$ versus vector group.

biofunctions of cancer cells via sponging miRNAs [19,23,32]. To elucidate whether *circNR3C1* possessed same mechanism in bladder cancer cells, we designed pull-down assay with specific *circNR3C1* probe (Fig. 4A), and then used StarBase prediction software to screen 11 candidate miRNAs that might be bound by *circNR3C1* with the specific target sites [33]. As shown in Fig. 4B, the efficiency and specific of this pull-down assay were verified by the results that *circNR3C1*, but not NR3C1 mRNA, could be abundantly pulled down by *circNR3C1* probe, and were further confirmed upon *circNR3C1* overexpression (Fig. 4C). Then, the relative levels of the 11 candidate miRNAs were evaluated. The results showed that miR-27a-3p, miR-23a-3p and miR-421 could be efficiently pulled down by *circNR3C1* in EJ cells. Meanwhile, miR-27a-3p, miR-23a-3p, and miR-942-5p were significantly enriched in *circNR3C1*-overexpressed EJ cells (Fig. 4D). Furthermore, only miR-23a-3p and miR-27a-3p were consistently pulled down both in vector control and *circNR3C1* overexpression plasmid transfectants (Fig. 4E). Taken together, these results suggested that miR-23a-3p, or miR-27a-3p, might be involved in *circNR3C1*-induced inhibition of bladder cancer cell proliferation.

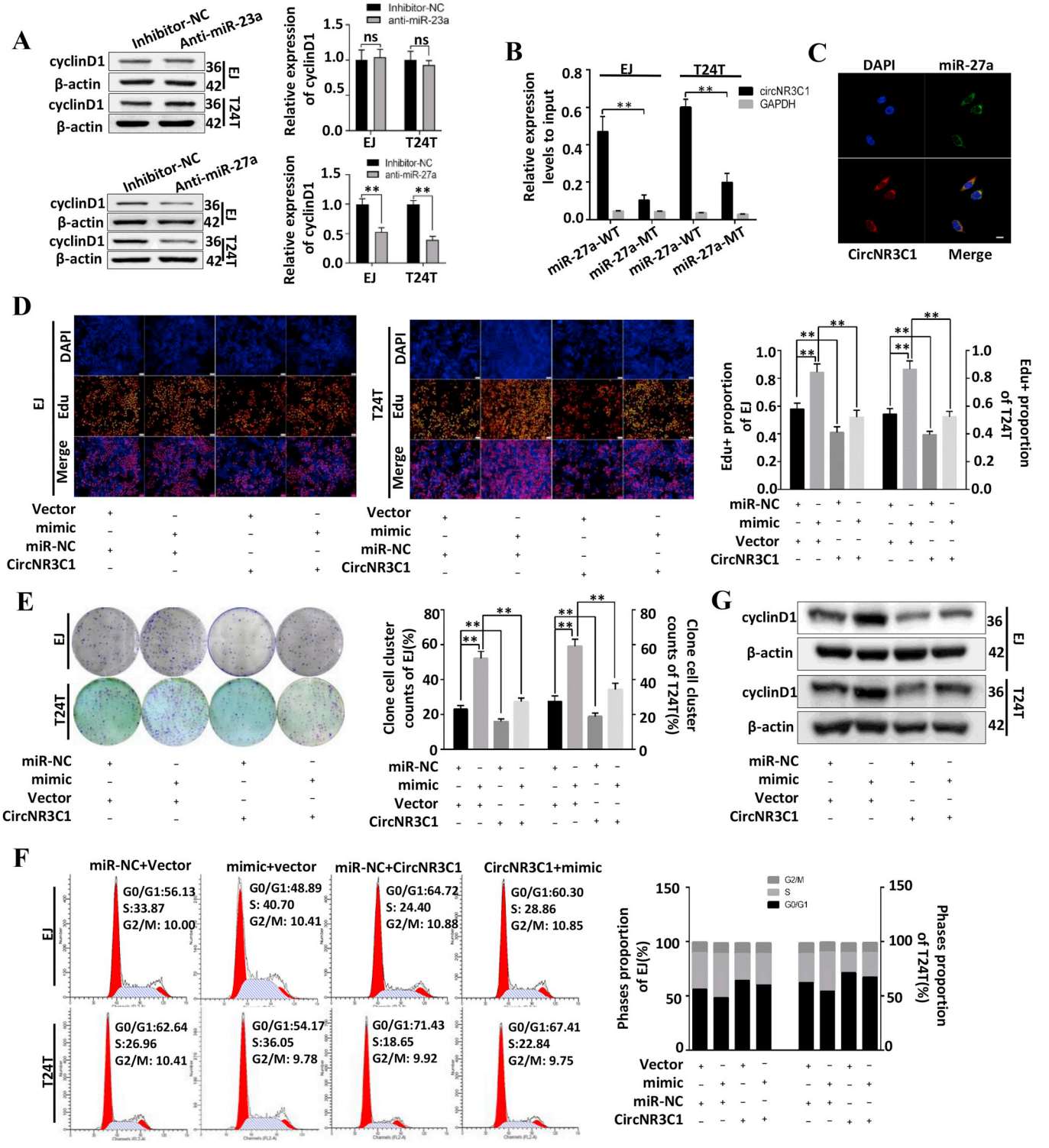

(caption on next page)

3.5. CircNR3C1 directly sponges miR-27a-3p to downregulate cyclin D1 expression and inhibit cell cycle progression and cell proliferation

To figure out whether miR-23a-3p, or miR-27a-3p, exhibits effect on expression of cyclin D1, miR-23a-3p and miR-27a-3p inhibitors were respectively used (Fig. S1B and Fig. S1C). It showed that the protein level of cyclin D1 was down-regulated in bladder cancer cells transfected with miR-27a-3p inhibitors compared with negative controls (inhibitor-NC), while transfection of miR-23a-3p didn't affect cyclin D1 expression (Fig. 5A). Besides, we found that *circNR3C1* harbored 4 predictive binding sites of miR-27a-3p ($\Delta G < -19.0$ kcal/mol), which were analyzed through predictive tool RNAhybrid [34](Fig. S3A and Fig. S3B). To further demonstrate the direct interaction between miR-27a-3p and *circNR3C1*, we designed wildtype biotin-miR-27a-3p (WT) and mutant type biotin-miR-27a-3p (MT) (Fig. S3C), and performed biotin-miR-27a-3p pull-down assay. As shown in Fig. 5B, a significantly higher enrichment of *circNR3C1* was captured in wild type biotin-miR-27a-3p-transfected cells than mutant type biotin-miR-27a-3p

Fig. 5. *circNR3C1* sponges miR-27a-3p to downregulate cyclin D1 expression and inhibits cell cycle progression and proliferation. (A) Western blot was performed to detect the expression of cyclin D1 in EJ and T24T cells which were transfected with miR-23a-3p inhibitors or miR-27a-3p inhibitors for 48 h and the relative expression level of cyclin D1 were calculated to do statistical analysis. Inhibitor negative control (Inhibitors-NC) was used as control. The results were derived from three independent experiments. Data are mean ± SEM, n = 3, $^{**}P < 0.01$. ^{ns} P > 0.05 (B) The biotinylated wild-type miR-27a-3p (miR-27a-WT) or its mutant (miR-27a-MT) was transfected into EJ and T24T cells for 48 h. *CircNR3C1* expression levels were quantified by qRT-PCR, and the relative expression level of *circNR3C1* to input was exhibited. *GAPDH* was used as negative control. Wild-type and mutant sequences of biotin-miR-27a-3p are shown in Fig. S3C. Data are mean ± SEM, n = 3, $^{**}P < 0.01$. (C) FISH assay showed the co-localization between *circNR3C1* and miR-23a-3p in T24T cells. *circNR3C1* probes were labeled with Cy3. MiR-27a-3p probes were labeled with FAM. Nucleus were stained with DAPI. Scale bar, 10 μm. (D) EdU assay showed the proliferation of EJ and T24T cells which co-transfected with *circNR3C1* control (vector) or *circNR3C1* plasmid, and miR-27a-3p negative control (miR-NC) or miR-27a-3p mimics (mimic) for 48 h. The data indicated mean ± SEM, n = 3, $^{**}P < 0.01$. (E) Colony formation assay showed the colony formation efficiency of EJ and T24T cells which co-transfected with *circNR3C1* control (vector) or *circNR3C1* plasmid, and miR-27a-3p miR-NC or miR-27a-3p mimics for 48 h. The data indicated mean ± SEM, n = 3, $^{**}P < 0.01$. (F) The cell cycle analysis showed cell counts and proportion of each phase in EJ and T24T cells which co-transfected with *circNR3C1* control (vector) or *circNR3C1* plasmid, and miR-NC or miR-27a-3p mimics for 48 h. The data indicated mean ± SEM, n = 3, $^{**}P < 0.01$. (G) Western blot assay was performed to detect the expression of cyclin D1 in EJ and T24T cells which co-transfected with *circNR3C1* control (vector) or *circNR3C1* plasmid, and miR-NC or miR-27a-3p mimics for 48 h. The results were derived from three independent experiments.

transfectants. Meanwhile, RNA fluorescence in situ hybridization (FISH) assay revealed that *circNR3C1* and miR-27a-3p were co-localized in cytoplasm (Fig. 5C). Next, to confirm the biofunction of miR-27a-3p in bladder cancer cells, cell cycle assay, colony formation assay and EdU assay were carried out. As shown in Fig. 5D and E, overexpression of miR-27a-3p could significantly promote cell proliferation of bladder cancer cells. Moreover, the enhancement of cell proliferation induced by miR-27a-3p could partly be reversed by overexpression of *circNR3C1*. Furthermore, flow cytometry assay demonstrated that overexpression of miR-27a-3p could stimulate the transition of bladder cancer cells from G0/G1 to S phase, and was partly compromised by enforced expression of *circNR3C1* (Fig. 5F). Additionally, western blot assay showed that miR-27a-3p induction of cyclin D1 expression was also significantly suppressed upon *circNR3C1* overexpression (Fig. 5G). These evidences suggested that overexpression of *circNR3C1* suppressed cyclin D1 expression by sponging miR-27a-3p to induce cell cycle arrest at G0/G1 phase, and subsequently inhibited proliferation of bladder cancer cells.

3.6. miR-27a-3p directly targets 5' UTR of cyclin D1 to promote its expression

To clarify how miR-27a-3p promoted the expression of cyclin D1, the mRNA expression level of cyclin D1 was detected in bladder cancer cells transfected with *circNR3C1* or miR-27a-3p inhibitors. However, the result showed that cyclin D1 mRNA levels were not affected by *circNR3C1* or miR-27a-3p inhibitors (Fig. 6A–B). It has been demonstrated that miRNA could directly up-regulate expression of target gene by targeting mRNA 5′UTR [35]. Importantly, we found that 5′UTR of cyclin D1 harbored two potential miR-27a-3p binding sites according to predict tool RNAhybrid [34] (Fig. 6C). Accordingly, the luciferase activity of cyclin D1 5′UTR was dramatically decreased in bladder cancer cells transfected with *circNR3C1* overexpression plasmid or miR-27a-3p inhibitors (Fig. 6D–E), which indicated that miR-27a-3p promoted cyclin D1 expression by targeting 5′UTR of cyclin D1. To further verify the molecular mechanism, three mutants of cyclin D1 5′ UTR were designed to perform luciferase reporter assay according to predictive miR-27a-3p binding sites (Fig. 6F). As shown in Fig. 6G–H, the luciferase activity of cyclin D1 5′ UTR showed no change upon transfection of *circNR3C1* overexpression plasmid or miR-27a-3p inhibitors while the first one of the indicated binding site was mutated, suggesting that this site was the functional locus that miR-27a-3p bound to the cyclin D1 5′UTR. To further confirm the effect of interaction between *circNR3C1* and miR-27a-3p on regulating cyclin D1 expression, miR-27a-3p mimics and *circNR3C1* were co-transfected into EJ and T24T cells. It showed that overexpression of miR-27a-3p mimics could partially reverse the *circNR3C1*-mediated suppression of cyclin D1 5′UTR activity (Fig. 6I). We subsequently analyzed the Initiating Ribosomes binding sites in cyclin D1 mRNA 5′-UTR using a ribo-seq genome browser (GWIPS-viz). The result showed that miR-27a-3p-targeted functional site was located outside the Initiating Ribosomes binding region (Fig. S5). Hence, we concluded that *circNR3C1* suppressed cyclin D1 expression via sponging miR-27a-3p to decrease interactions between miR-27a-3p and the 5′UTR of cyclin D1.

4. Discussion

Urothelial bladder cancer is a heterogeneous epithelial malignancy disease that undergoes a variety of clinical courses and possesses diverse therapeutic responses, and specific therapeutic strategies should be investigated for the close association between its molecular subtypes and clinicopathological features [2,36]. Several studies have shown that the expression profiles of circRNAs are aberrant in diverse cancer types and some of them play very important roles in oncogenesis and cancer development [37]. Previously, we have reported that *circHIPK3* sponged miR-558 and suppressed heparanase expression to impair bladder cancer cell invasion [23], circRNA *BCRC-3* inhibited bladder cancer cell proliferation through increasing the expression of p27 [38], and circRNA *BCRC4* promoted apoptosis by up-regulating the expression of miR-101 [39]. In this study, we found that *circNR3C1* was down-regulated in bladder cancer tissues and cells compared to normal bladder tissues and cells. It was shown that there was no significant difference of *circNR3C1* expression between the two invasive bladder cancer cells (UMUC3, J82) and the superficial non-invasive bladder cancer cells (5637), indicating there was no clear correlation between expression of *circNR3C1* and aggressiveness of the cell line. Accordingly, there was no correlation between *circNR3C1* and the clinicopathological including stage, pTNM, invasion and metastasis in the bladder cancer tissues. Nevertheless, enforced expression of *circNR3C1* could inhibit proliferation of muscle invasive bladder cancer cells, and the metastatic T24T cells were more responsive, indicating that *circNR3C1* might be a potential therapeutic target in progressive bladder cancer.

Early studies had reported that circRNAs could function as efficient miRNA sponges [13]. However, circRNAs also possessed some other biofunctions except "miRNA sponges". *CircMBL* and its franking introns could be strongly and specifically bound by MBL, which contributed to the biogenesis of circRNAs [40]. *CircFoxo3* promoted MDM2-induced p53 ubiquitination and subsequent degradation by binding to p53 and *MDM2*, which indicate that circRNAs may function as protein scaffolds [41]. Recently, it was reported that *circ-ZNF609* could be translated to a protein in a cap-independent manner in eukaryote [42]. In the present study, *circNR3C1* was found located at cytoplasm, and multiple miRNA-binding sites were predicted in its sequences by miRNA response elements (MREs) analysis, indicating that *circNR3C1* might function as a miRNA sponge. Actually, our data clarified that *circNR3C1* harbored four miRNA binding sites of miR-27a-3p and could sponge miR-27a-3p as competing endogenous RNA in bladder cancer cells, which further verified "miRNA sponges" theory. However, whether *circNR3C1* possesses other functions in biological process, such as translation or

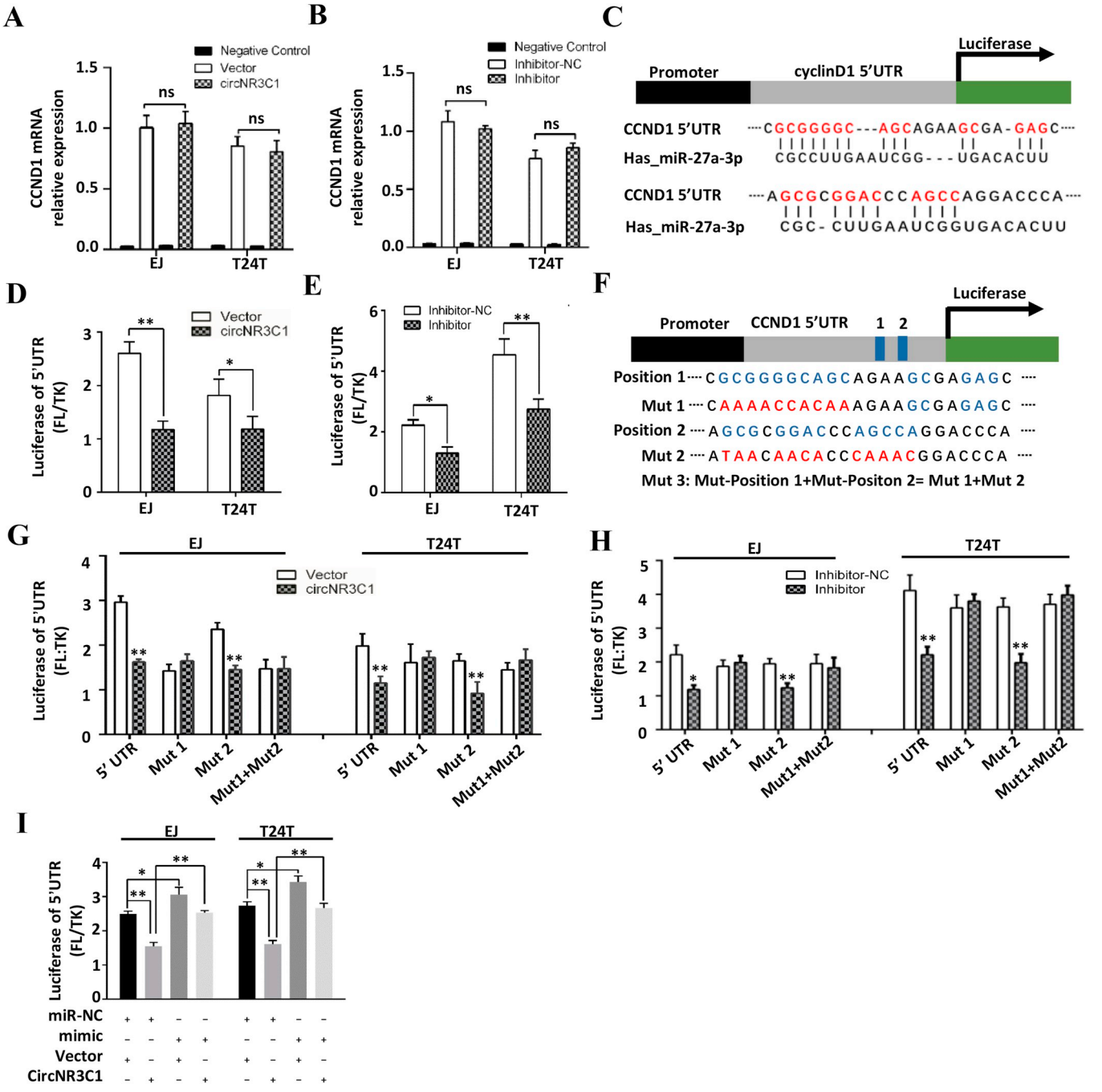

Fig. 6. *cyclin D1* is directly targeted by miR-27a-3p. (A–B) cyclin D1 mRNA expression level was measured using qRT-PCR in EJ and T24T cells which were transfected with *circNR3C1* plasmid or *circNR3C1* control (vector), and miR-27a-3p-inhibtors or inhibitor NC for 48 h. The negative control was used to rule out the genomic DNA amplification. The data indicated mean ± SEM, n = 3, ns > 0.05. **(C)** Schematic diagram showed the structure of dual luciferase reporter plasmid of *cyclin D1* 5′UTR and putative binding sites of cyclin D1 5′UTR bound by miR-27a-3p, as predicted by RNAhybrid2.2. **(D–E)** Dual luciferase reporter assay showed that luciferase activities were significantly decreased in EJ and T24T cells after transfected with *circNR3C1* or miR-27a-3p-inhibitors compared with controls for 48 h. The data indicated mean ± SEM, n = 3, *p < 0.05, **p < 0.01. (F) Three mutants (Mut 1, Mu2 and Mut 1 + Mut2) of dual luciferase reporter plasmids were designed to confirm the two candidates (position 1 and position 2) of miR-27a-3p binding sites of *cyclin D1* 5′UTR as shown in schematic figure. The bases colored with blue were replace by the bases colored with red in synthesizing the mutants. **(G–H)** The luciferase activities of *cyclin D1* 5′UTR were measured in EJ and T24T cells which co-transfected with *circNR3C1* plasmid or miR-27a-3p-inhibitors, and three mutants or 5′UTR plasmid for 48 h, respectively. The data indicated mean ± SEM, n = 3. *p < 0.05 versus vector, **p < 0.01 versus vector. **(I)** The luciferase activities of cyclin D1 5′UTR were measured in EJ and T24T cells which co-transfected with *circNR3C1* plasmid or vectors, and miR-27a-3p mimic or miR-NC for 48 h. The data indicated mean ± SEM, n = 3. *p < 0.05, **p < 0.01.

protein sponge, still needs to be explored.

An increasing number of evidences suggest that microRNAs are abnormally expressed in diverse human cancers and have important roles in the tumorigenesis, progression and metastasis of these cancers [43]. Several studies have demonstrated that miR-27a-3p was upregulated and played significant roles in promoting cell proliferation, migration, invasion and metastatic in multiple types of cancers, such as human gastric cancer [44], breast cancer [45], and renal cell carcinoma [46]. Our recent study indicated that inhibition of miR-27a-3p by *MEG3*, a competing endogenous RNA, could promote PHLPP2 protein

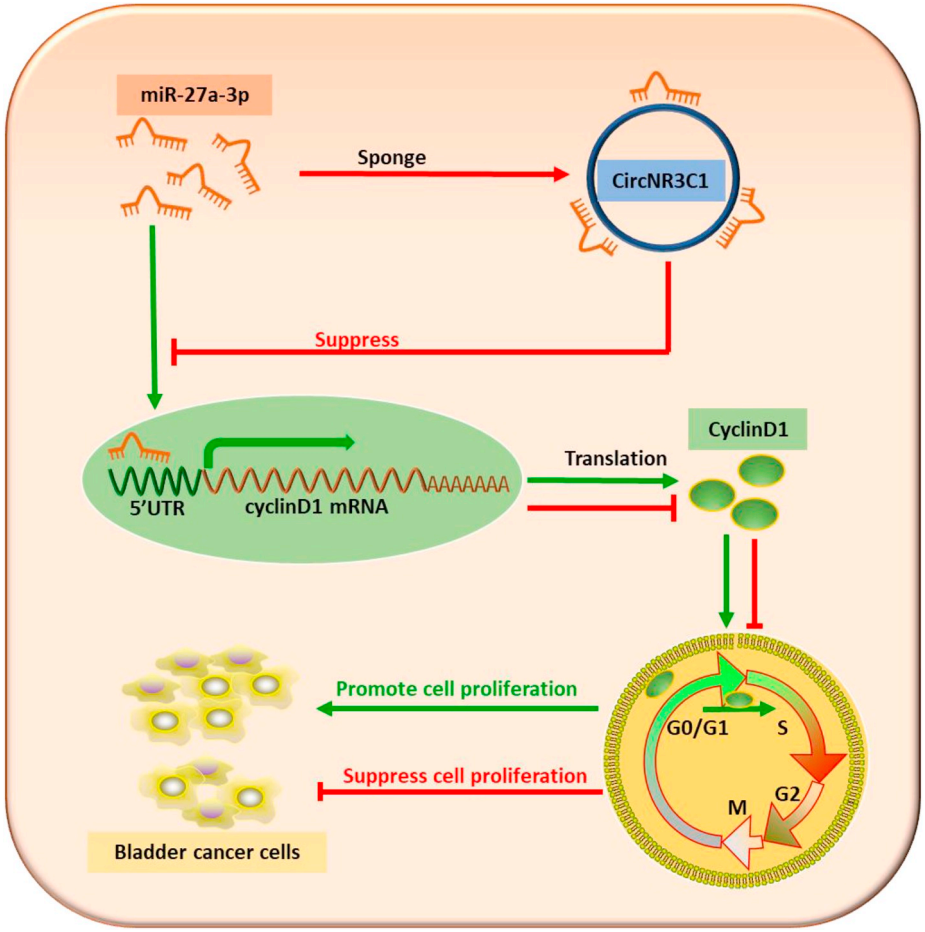

Fig. 7. Schematic diagram of the *circNR3C1*-regulated pathway in bladder cancer cells. The green arrows indicate promotive function and red lines indicate suppressive function. (For interpretation of the references to color in this figure legend, the reader is referred to the Web version of this article.)

translation and impair bladder cancer cell invasion [47]. Previously, up-regulation of miR-27a-3p under hypoxia has been demonstrated to confer high risk of high-grade human bladder cancer [48]. On the other hand, it has been reported that downregulation of miR-27a-3p in the serum of human bladder cancer patients correlated with higher tumor grade [49]. In addition, miR-27a-3p has been confirmed to increase the chemo-sensitivity of bladder cancer through upregulating the expression of *RUNX-1* [50]. Nevertheless, the exact roles of miR-27a-3p in bladder cancer progression still need to be clarified. Our study showed that overexpression of miR-27a-3p promoted cell cycle progression and proliferation of bladder cancer cells, which suggested that miR-27a-3p played a role as an oncogene in regulating bladder cancer cell proliferation.

In general, miRNAs regulate gene expression upon post-transcription in animal predominantly via base pairing incompletely to the 3′ UTR of target mRNAs and affect protein synthesis or mRNA levels [51]. Nevertheless, several studies have revealed that miRNAs may regulate gene expression by binding to 5′ UTRs of target genes. It has been reported that miRNAs could target the 5′-UTR of mRNA to increase its secondary structure stability [52], and miRNAs has also been proved to directly bind to the 5′-UTR of mRNA to enhance its translation [35]. In our study, we found that miRNA-27a-3p targeted 5′-UTR of cyclin D1 mRNA and upregulated its expression at protein level, while the mRNA level of cyclin D1 was not changed, indicating that miRNA-27a-3p could promote cyclin D1 translation. It was reported that the translation of the cyclin D1 occurred via internal ribosome entry site (IRES)-mediated initiation in its mRNA 5′-UTR [53]. However, our studies showed that miR-27a-3p-targeted functional site was located outside the Initiating Ribosomes binding region, suggesting that the interaction of miR-27a-3p with cyclin D1 mRNA 5′-UTR might facilitate the nearby Initiating Ribosomes binding, rather than formed a tertiary structure.

Although our study confirmed that *circNR3C1* played a role in inhibiting the cell proliferation in vitro and tumor growth in vivo through sponging miR-27a-3p and suppressing cyclin D1 expression, it was still unclear whether *circNR3C1* may act as an anti-oncogene through other pathway such as immunological regulation. It was reported that evading of immune surveillance plays important roles in bladder cancer progression [54], immunological effect might be involved in the reason why tumors were more affected by circNR3C1 than the cell lines.

In conclusion, we reveal that *circNR3C1* is significantly down-regulated in bladder cancer tissues and cell lines, and it suppresses cell cycle progression by directly sponging miR-27a-3p to block its interaction with cyclin D1 mRNA 5′UTR, and subsequently inhibits cyclin D1 expression to impair proliferation of bladder cancer cells (Fig. 7).

Conflicts of interest

The authors have declared that no conflict interests exist.

Acknowledgments

This work was supported by the National Natural Science Foundation of China (No. 81672529, 81772724, 81702524, 81472406, 81402113, 81602234, 81802559).

Appendix A. Supplementary data

Supplementary data to this article can be found online at https://

doi.org/10.1016/j.canlet.2019.06.018.

References

[1] S. Antoni, J. Ferlay, I. Soerjomataram, A. Znaor, A. Jemal, F. Bray, Bladder cancer incidence and mortality: a global overview and recent trends, Eur. Urol. 71 (1) (2017) 96–108.

[2] I. K, Bladder cancer: new insights into its molecular pathology, Cancers 10 (4) (2018) (undefined).

[3] H. Sanger, G. Klotz, D. Riesner, H. Gross, A. Kleinschmidt, Viroids are single-stranded covalently closed circular RNA molecules existing as highly base-paired rod-like structures, Proc. Natl. Acad. Sci. U.S.A. 73 (11) (1976) 3852–3856.

[4] A. Kos, R. Dijkema, A.C. Arnberg, P.H. van der Meide, H. Schellekens, The hepatitis delta (delta) virus possesses a circular RNA, Nature 323 (6088) (1986) 558–560.

[5] M.T. Hsu, M. Coca-Prados, Electron microscopic evidence for the circular form of RNA in the cytoplasm of eukaryotic cells, Nature 280 (5720) (1979) 339–340.

[6] C. Cocquerelle, P. Daubersies, M.A. Majerus, J.P. Kerckaert, B. Bailleul, Splicing with inverted order of exons occurs proximal to large introns, EMBO J. 11 (3) (1992) 1095–1098.

[7] J.M. Nigro, K.R. Cho, E.R. Fearon, S.E. Kern, J.M. Ruppert, J.D. Oliner, et al., Scrambled exons, Cell 64 (3) (1991) 607–613.

[8] B. Capel, A. Swain, S. Nicolis, A. Hacker, M. Walter, P. Koopman, et al., Circular transcripts of the testis-determining gene Sry in adult mouse testis, Cell 73 (5) (1993) 1019–1030.

[9] C. Cocquerelle, B. Mascrez, D. Hetuin, B. Bailleul, Mis-splicing yields circular RNA molecules, FASEB J. 7 (1) (1993) 155–160.

[10] J. Salzman, R.E. Chen, M.N. Olsen, P.L. Wang, P.O. Brown, Cell-type specific features of circular RNA expression, PLoS Genet. 9 (9) (2013) e1003777.

[11] J.O. Westholm, P. Miura, S. Olson, S. Shenker, B. Joseph, P. Sanfilippo, et al., Genome-wide analysis of drosophila circular RNAs reveals their structural and sequence properties and age-dependent neural accumulation, Cell Rep. 9 (5) (2014) 1966–1980.

[12] X. Fan, X. Zhang, X. Wu, H. Guo, Y. Hu, F. Tang, et al., Single-cell RNA-seq transcriptome analysis of linear and circular RNAs in mouse preimplantation embryos, Genome Biol. 16 (2015) 148.

[13] T.B. Hansen, T.I. Jensen, B.H. Clausen, J.B. Bramsen, B. Finsen, C.K. Damgaard, et al., Natural RNA circles function as efficient microRNA sponges, Nature 495 (7441) (2013) 384–388.

[14] W. Jeck, J. Sorrentino, K. Wang, M. Slevin, C. Burd, J. Liu, et al., Circular RNAs are abundant, conserved, and associated with ALU repeats, RNA 19 (2) (2013) 141–157.

[15] S. Kelly, C. Greenman, P. Cook, A. Papantonis, Exon skipping is correlated with exon circularization, J. Mol. Biol. 427 (15) (2015) 2414–2417.

[16] X.O. Zhang, H.B. Wang, Y. Zhang, X. Lu, L.L. Chen, L. Yang, Complementary sequence-mediated exon circularization, Cell 159 (1) (2014) 134–147.

[17] S. Memczak, M. Jens, A. Elefsinioti, F. Torti, J. Krueger, A. Rybak, et al., Circular RNAs are a large class of animal RNAs with regulatory potency, Nature 495 (7441) (2013) 333–338.

[18] A. Rybak-Wolf, C. Stottmeister, P. Glazar, M. Jens, N. Pino, S. Giusti, et al., Circular RNAs in the mammalian brain are highly abundant, conserved, and dynamically expressed, Mol. Cell 58 (5) (2015) 870–885.

[19] L. Chen, S. Zhang, J. Wu, J. Cui, L. Zhong, L. Zeng, et al., circRNA_100290 plays a role in oral cancer by functioning as a sponge of the miR-29 family, Oncogene 36 (32) (2017) 4551–4561.

[20] J. Zheng, X. Liu, Y. Xue, W. Gong, J. Ma, Z. Xi, et al., TTBK2 circular RNA promotes glioma malignancy by regulating miR-217/HNF1beta/Derlin-1 pathway, J. Hematol. Oncol. 10 (1) (2017) 52.

[21] D. Han, J. Li, H. Wang, X. Su, J. Hou, Y. Gu, et al., Circular RNA circMTO1 acts as the sponge of microRNA-9 to suppress hepatocellular carcinoma progression, Hepatology 66 (4) (2017) 1151–1164.

[22] K.Y. Hsiao, Y.C. Lin, S.K. Gupta, N. Chang, L. Yen, H.S. Sun, et al., Noncoding effects of circular RNA CCDC66 promote colon cancer growth and metastasis, Cancer Res. 77 (9) (2017) 2339–2350.

[23] Y. Li, F. Zheng, X. Xiao, F. Xie, D. Tao, C. Huang, et al., CircHIPK3 sponges miR-558 to suppress heparanase expression in bladder cancer cells, EMBO Rep. 18 (9) (2017) 1646–1659.

[24] R. Carthew, E. Sontheimer, Origins and Mechanisms of miRNAs and siRNAs, Cell 136 (4) (2009) 642–655.

[25] H. Yoshino, N. Seki, T. Itesako, T. Chiyomaru, M. Nakagawa, H. Enokida, Aberrant expression of microRNAs in bladder cancer, Nat. Rev. Urol. 10 (7) (2013) 396–404.

[26] Z. Zhong, M. Huang, M. Lv, Y. He, C. Duan, L. Zhang, et al., Circular RNA MYLK as a competing endogenous RNA promotes bladder cancer progression through modulating VEGFA/VEGFR2 signaling pathway, Cancer Lett. 403 (2017) 305–317.

[27] G. JJ, G. WL, H. MA, T. D, Genetic and phenotypic changes associated with the acquisition of tumorigenicity in human bladder cancer, Genes Chromosomes Cancer 27 (3) (2000) 252–263.

[28] K. Wang, B. Long, F. Liu, J. Wang, C. Liu, B. Zhao, et al., A circular RNA protects the heart from pathological hypertrophy and heart failure by targeting miR-223, Eur. Heart J. 37 (33) (2016) 2602–2611.

[29] D. Liu, Y. Li, G. Luo, X. Xiao, D. Tao, X. Wu, et al., LncRNA SPRY4-IT1 sponges miR-101-3p to promote proliferation and metastasis of bladder cancer cells through up-regulating EZH2, Cancer Lett. 388 (2017) 281–291.

[30] G. Jiang, C. Huang, J. Li, H. Huang, H. Jin, J. Zhu, et al., Role of STAT3 and FOXO1 in the divergent therapeutic responses of non-metastatic and metastatic bladder cancer cells to miR-145, Mol. Cancer Ther. 16 (5) (2017) 924–935.

[31] W.R. Jeck, N.E. Sharpless, Detecting and characterizing circular RNAs, Nat. Biotechnol. 32 (5) (2014) 453–461.

[32] Q. Zheng, C. Bao, W. Guo, S. Li, J. Chen, B. Chen, et al., Circular RNA profiling reveals an abundant circHIPK3 that regulates cell growth by sponging multiple miRNAs, Nat. Commun. 7 (2016) 11215.

[33] J. Li, S. Liu, H. Zhou, L. Qu, J. Yang, starBase v2.0: decoding miRNA-ceRNA, miRNA-ncRNA and protein-RNA interaction networks from large-scale CLIP-Seq data, Nucleic Acids Res. 42 (2014) D92–D97 Database issue.

[34] J. Krüger, M. Rehmsmeier, RNAhybrid: microRNA target prediction easy, fast and flexible, Nucleic Acids Res. 34 (2006) W451–W454 Web Server issue.

[35] U. Ørom, F. Nielsen, A. Lund, MicroRNA-10a binds the 5'UTR of ribosomal protein mRNAs and enhances their translation, Mol. Cell 30 (4) (2008) 460–471.

[36] A.G. Robertson, J. Kim, H. Al-Ahmadie, J. Bellmunt, G. Guo, A.D. Cherniack, et al., Comprehensive molecular characterization of muscle-invasive bladder cancer, Cell 174 (4) (2018) 1033.

[37] L.S. Kristensen, T.B. Hansen, M.T. Veno, J. Kjems, Circular RNAs in cancer: opportunities and challenges in the field, Oncogene 37 (5) (2018) 555–565.

[38] F. Xie, Y. Li, M. Wang, C. Huang, D. Tao, F. Zheng, et al., Circular RNA BCRC-3 suppresses bladder cancer proliferation through miR-182-5p/p27 axis, Mol. Cancer 17 (1) (2018) 144.

[39] B. Li, F. Xie, F. Zheng, G. Jiang, F. Zeng, X. Xiao, Overexpression of CircRNA BCRC4 regulates cell apoptosis and MicroRNA-101/EZH2 signaling in bladder cancer, J. Huazhong Univ. Sci. Technol. - Med. Sci. 37 (6) (2017) 886–890.

[40] R. Ashwal-Fluss, M. Meyer, N.R. Pamudurti, A. Ivanov, O. Bartok, M. Hanan, et al., circRNA biogenesis competes with pre-mRNA splicing, Mol. Cell 56 (1) (2014) 55–66.

[41] W.W. Du, L. Fang, W. Yang, N. Wu, F.M. Awan, Z. Yang, et al., Induction of tumor apoptosis through a circular RNA enhancing Foxo3 activity, Cell Death Differ. 24 (2) (2017) 357–370.

[42] I. Legnini, G. Di Timoteo, F. Rossi, M. Morlando, F. Briganti, O. Sthandier, et al., Circ-ZNF609 is a circular RNA that can Be translated and functions in myogenesis, Mol. Cell 66 (1) (2017) 22–37 e9.

[43] K.M. Nelson, G.J. Weiss, MicroRNAs and cancer: past, present, and potential future, Mol. Cancer Ther. 7 (12) (2008) 3655–3660.

[44] L. Zhou, X. Liang, L. Zhang, L. Yang, N. Nagao, H. Wu, et al., MiR-27a-3p functions as an oncogene in gastric cancer by targeting BTG2, Oncotarget 7 (32) (2016) 51943–51954.

[45] S.U. Mertens-Talcott, S. Chintharlapalli, X. Li, S. Safe, The oncogenic microRNA-27a targets genes that regulate specificity protein transcription factors and the G2-M checkpoint in MDA-MB-231 breast cancer cells, Cancer Res. 67 (22) (2007) 11001–11011.

[46] H. Peng, X. Wang, P. Zhang, T. Sun, X. Ren, Z. Xia, miR-27a promotes cell proliferation and metastasis in renal cell carcinoma, Int. J. Clin. Exp. Pathol. 8 (2) (2015) 2259–2266.

[47] H. C, L. X, J. H, X. F, Z. F, L. J, et al., MEG3, as a competing endogenous RNA, binds with miR-27a to promote PHLPP2 protein translation and impairs bladder cancer invasion, Mol. Ther. Nucleic Acids 16 (undefined) (2019) 51–62.

[48] X. Y, Z. M, W. J, Z. Y, L. S, Z. B, et al., Role of microRNA-27a in down-regulation of angiogenic factor AGGF1 under hypoxia associated with high-grade bladder urothelial carcinoma, Biochim. Biophys. Acta 1842 (5) (2014) 712–725.

[49] X. Jiang, L. Du, L. Wang, J. Li, Y. Liu, G. Zheng, et al., Serum microRNA expression signatures identified from genome-wide microRNA profiling serve as novel non-invasive biomarkers for diagnosis and recurrence of bladder cancer, Int. J. Cancer 136 (4) (2015) 854–862.

[50] Y. Deng, H. Bai, H. Hu, G/A variation in miR-27a decreases chemo-sensitivity of bladder cancer by decreasing miR-27a and increasing the target RUNX-1 expression, Biochem. Biophys. Res. Commun. 458 (2) (2015) 321–327 rs11671784.

[51] R.S. Pillai, S.N. Bhattacharyya, W. Filipowicz, Repression of protein synthesis by miRNAs: how many mechanisms? Trends Cell Biol. 17 (3) (2007) 118–126.

[52] G. W, X. Y, X. X, W. T, K. JH, Z. T, The role of RNA structure at 5' untranslated region in microRNA-mediated gene regulation, RNA 20 (9) (2014) 1369–1375.

[53] H. B, L. J, L. KA, B.-S. A, B. T, J. ME, et al., Mechanistic target of Rapamycin (mTOR) inhibition synergizes with reduced internal ribosome entry site (IRES)-mediated translation of cyclin D1 and c-MYC mRNAs to treat glioblastoma, J. Biol. Chem. 291 (27) (2016) 14146–14159.

[54] N. R, B. J, Management of metastatic bladder cancer, Cancer Treat Rev. 76 (2019) 10–21 undefined.